

PREPARATION AND CHARACTERIZATION OF TiO₂-CHITOSAN COMPOSITE FILMS AND APPLICATION FOR TARTRAZINE DYE DEGRADATION

DJAMILA ZIOUI,* LAMINE AOUDJIT,* FOUZIA TOUAHRA** and KHALDOUN BACHARI**

**Unité de Développement des Équipements Solaires, UDES/Centre de Développement
des Energies Renouvelables, CDER, Bou Ismail, 42415, W. Tipaza, Algeria*

***Centre de Recherche Scientifique et Technique en Analyses Physico-chimiques (CRAPC),
BP 384 Bou Ismail, RP42004, Tipaza, Algeria*

✉ Corresponding author: L. Aoudjit, lamineaoudjit@yahoo.fr

Received June 6, 2022

The aim of this work was to synthesize nanocomposite membranes based on chitosan (CS) biopolymer containing TiO₂ nanoparticles (TiO₂-Chitosan). The developed membranes were fully featured using different characterization techniques (SEM, TGA, XRD, FTIR and contact angle measurement). The photocatalytic activity of the fabricated membranes was evaluated by performing experiments in which aqueous solutions of tartrazine dye that contained the fabricated membrane were irradiated with solar light. The photodegradation percentage was spectrophotometrically determined by monitoring the maximum wavelengths (λ_{max}) of tartrazine at 427 nm for different irradiation times. The decolourisation percentage of the dye under solar light was 83% using the TiO₂-Chitosan membrane. The effective reusability and stability of the produced nanocomposite (TiO₂-Chitosan) films was also assessed. After four use cycles, this efficiency remained practically constant, demonstrating the membranes' reusability and suitability for catalytic activity in tartrazine removal from water.

Keywords: chitosan membrane, TiO₂ nanocomposite, tartrazine dye, water and wastewater treatment

INTRODUCTION

Water pollution generated from organic dye contaminants has become an increasing global environmental concern in recent years. Organic dyes are mainly produced from manufacturing activities, such as textile finishing, plastics, paper, cosmetics, pharmaceuticals, and food processing.^{1,2} It can cause serious problems for both the environment and the human beings. Tartrazine (C.I. Acid Yellow 23, AY23) was selected as a pollutant model for the present work. Tartrazine is an azoic dye widely used in the textile, cosmetics, pharmaceutical and food industries.³ The acidic azo dye, tartrazine, has a sulfonic group as an auxochrome that makes it highly water soluble and most refractory to biodegradation. Many studies published in the last few decades have reported the dangers of tartrazine dye at higher concentrations (4 and 8 mM), identifying its potentially deleterious effects, such as food allergies, mutagenicity, carcinogenicity and phototoxicity.^{4,1-3}

Consequently, the wastewater containing tartrazine dye in various concentrations should be treated before discharge.

In this respect, several methods such as chemical oxidation, coagulation, adsorption, biodegradation, photocatalysis, reverse osmosis, and solar wastewater treatment (SOWAT) have been developed to treat dye-contaminated wastewater.^{5,1} In particular, photocatalysis is considered a "green" treatment method, which uses solar energy effectively for the degradation of organic pollutants.⁶⁻¹¹ Recently, titanium dioxide (TiO₂) has been found to be the most effective photocatalyst for wastewater applications.^{2,3} Due to its properties, such as low cost, abundance and non-toxicity, strong ultraviolet (UV) absorption, good physical and chemical stability in photocatalysis reactions and, commonly, energy band gap of 3.2eV, researches have demonstrated in recent works that the incorporation of TiO₂ into a polymeric matrix

provided a major stabilization of the semiconductor material (TiO_2), which resulted in higher pollutant degradation than in the case of the individual components, and resolved some drawbacks by the incorporation of TiO_2 into polymeric membranes related to its use in suspension, namely the recovery of solid particles.^{6,7} Various polymers have been used for the fabrication of membranes, among which cellulose acetate (CA), cellulose triacetate (CTA), poly(sulfone) (PSu), poly(ether sulfone) (PES), poly(vinylidene fluoride) (PVDF), poly(vinylidene fluoride-hexafluoropropylene) (PVDF-HFP), and copolymers, such as poly(vinylidene fluoride-trifluoroethylene) PVDF-TrFE.^{12,15} This wide variety of polymers, which define the chemical nature of the membrane, associated with multiple membrane geometries, makes it possible to manufacture membranes with different properties and are capable of covering various needs in several areas of use.

Chitosan (CS) is one of the most interesting biopolymers that is obtained from deacetylation of chitin and is considered to be the second most common natural polysaccharide.³ CS is particularly attractive due to its improved characteristics, such as high mechanical strength, excellent chemical resistance, natural abundance, non-toxicity, easy preparation, low cost, biodegradability, thermal stability, and biocompatibility. These properties make it suitable for several different applications (for example, as bio-adsorbents for wastewater treatment systems, for removing various pollutants, such as heavy metals, dyestuff, pathogens). The incorporation of a semiconductor (TiO_2) into the main constituent CS has modified the properties of the biopolymer, and the

biopolymer is expected to have broad applications.

The aim of the present work was to synthesize TiO_2 -Chitosan films and use them for the photocatalytic degradation of tartrazine dye under sunlight radiation. Finally, the effective reusability and stability of the produced nanocomposite (TiO_2 -Chitosan) films were also assessed.

EXPERIMENTAL

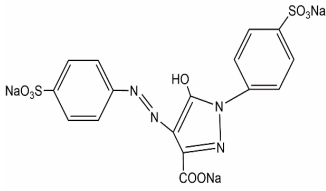
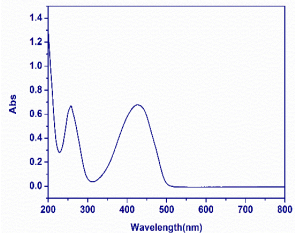
Materials

Chitosan was supplied by Pelican Biotech and Chemicals Labs, Kerala (India). Titanium dioxide was purchased from Sigma-Aldrich Co. Acetic acid (99.9% purity), and sodium hydroxide (98% purity) were purchased from Biochem Chemopharma. Tartrazine (Acid Yellow 23), a mono azo anionic dye, was obtained from ACROS Organics (U.S.A.). Its chemical structure and absorption spectrum are illustrated in Table 1. All solutions were prepared with ultrapure Milli-Q water (resistivity of 18.2 M Ω cm).

Synthesis of TiO_2 -chitosan films

A chitosan solution (CS) was prepared by solubilization in a 2% (v/v) acetic acid solution, as described by Aoudjit *et al.* in previous work.³ The CS solution was stirred at 30 °C until the chitosan had completely dissolved. The mixture was then stirred at 700 rpm for 3 hours at 30 °C with 0.4 g of TiO_2 nanoparticles. The formed solution was cast onto a Petri plate, and the film was obtained by the solvent evaporation method. Then, it was neutralized with sodium hydroxide (1M) and dried in an oven at 60 °C for 6 h to produce a TiO_2 -chitosan membrane. The characterization and photocatalytic activity of the prepared films were further evaluated. The pure chitosan film was prepared by the same procedure described above, but without the addition of TiO_2 nanopowder.

Table 1
Characteristics of the dye investigated in this study

Name of dye	Chemical structure	Type of dye	UV-vis absorption spectrum
Tartrazine Yellow 23		Anionic	
	Chemical formula	λ_{max} absorption (nm)	Molar mass, g/mol
	$\text{C}_{16}\text{H}_9\text{N}_4\text{Na}_3\text{O}_9\text{S}$	427	534.36

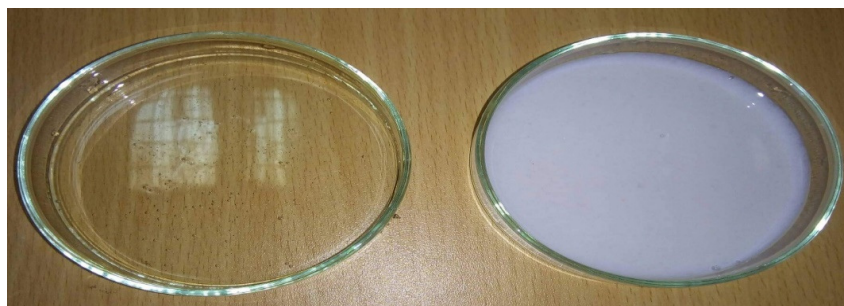


Figure 1: Photographs of prepared nanocomposite films: (a) Chitosan, (b) TiO₂-Chitosan

The pure chitosan films are transparent, and after the addition of TiO₂ nanopowder (Fig. 1), the prepared chitosan-TiO₂ films show increased whiteness and decreased transparency, which is consistent with the results reported in the work of Zhang *et al.*¹⁶

Film characterization

The crystal structure of the TiO₂-Chitosan film was evaluated by X-ray diffraction (XRD), using a Bruker D8 Discover diffractometer with incident CuK α radiation (40 kV and 30 mA). Fourier-transform infrared spectroscopy (FTIR) was performed to determine the chemical stability of the film, using an FTIR Alpha instrument (Bruker Corporation, Billerica, MA, U.S.A.), over a range of 500–4000 cm⁻¹, using 64 scans with a resolution of 4 cm⁻¹. Scanning electron microscopy (SEM) was carried out with a Quanta 650 SEM (Thermo Fisher, Waltham, MA, U.S.A.) to access the morphology and microstructure of the membrane. Thermogravimetric analysis (TGA) was performed using a specific apparatus (model Q500, TA Instruments). The thickness of the membranes was calculated using a digital micrometer. The density was determined by the pycnometer method and the water content was expressed as the ratio ranging from 0 (completely dry) to the value of the material porosity at saturation. Contact angle measurements were performed at room temperature in a Data Physics OCA20 device, using ultrapure water as test liquid. The optical properties of the TiO₂-Chitosan composite films were evaluated according to the light transmittance of the films. Film transmittance was measured at a wavelength of 600 nm using an ultraviolet (UV) spectrophotometer (Shimadzu UV1800).

RESULTS AND DISCUSSION

CS and TiO₂-Chitosan XRD patterns are shown in Figure 2. The peaks at $2\theta < 25^\circ$ are typical of chitosan (CS). Typical diffraction patterns of anatase and rutile (TiO₂) were also found at $2\theta^\circ$. These peaks are similar to the standard spectra (JCPDS card numbers: 88-1175 and 84-1286). An additional peak at 2θ of 20°

confirms the incorporation of TiO₂ into the structure of chitosan. These results are in good agreement with similar works.^{3,17}

The FTIR spectra of pure CS and TiO₂/chitosan membrane are shown in Figure 3. The wide band appearing at 3227.66 cm⁻¹ is attributed to the O-H stretching vibration of adsorbed water. The bands between 1574 and 1024 cm⁻¹ are related to the composition of chitosan. The peaks below 1000 cm⁻¹ were attributed to the Ti-O-Ti bond, the asymmetric stretching mode of Ti-O, and the immobilization of TiO₂ onto the CS matrix, which agrees with previous work.^{3,18-19}

The chitosan films revealed a smooth and flat surface, as shown in Figure 4 (a). The SEM images (Fig. 4 (b)) after TiO₂ incorporation into the chitosan matrix clearly show that the TiO₂ nanoparticles were mostly uniformly dispersed in the chitosan matrix, with some agglomerations. This result confirms the good dispersion of TiO₂ nanoparticles into the CS film. Similarly, Zhang *et al.*²⁰ performed SEM analysis on chitosan-TiO₂ composite films, and also reported that the TiO₂ nanopowder was successfully and uniformly dispersed into the chitosan matrix.

The thermogravimetric analysis (TGA) of pure CS and TiO₂-CS membranes was investigated (Fig. 5). The result showed the weight loss of the composite membrane (TiO₂-CS membrane) was comparatively lower than that of pure CS, suggesting less degradation potential and more thermal stability of the TiO₂-CS membrane, even at a higher temperature.

As observed from the values of the water content and contact angle in Table 2, it can be noticed that the developed membrane is hydrophilic (less than 90°). The values obtained for the thickness and density are quite comparable to those of the commercial supports used for the

preparation of membranes utilized in wastewater treatment activities. Transmittance measurements of the composite films showed that the transparency of the pure chitosan film was 54.95%, whereas that of composite films

containing TiO_2 was reduced, to 0.54%, respectively. This optical change was caused by high UV absorption and scattering induced by the presence of TiO_2 . These results are in harmony with a similar work reported by Zhang *et al.*¹⁶

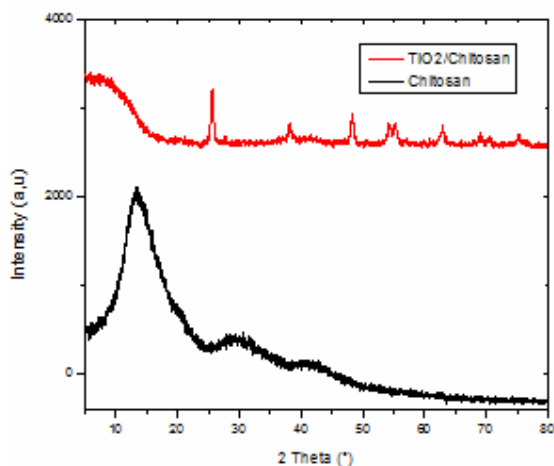


Figure 2: XRD patterns of chitosan film and chitosan composite film with TiO_2

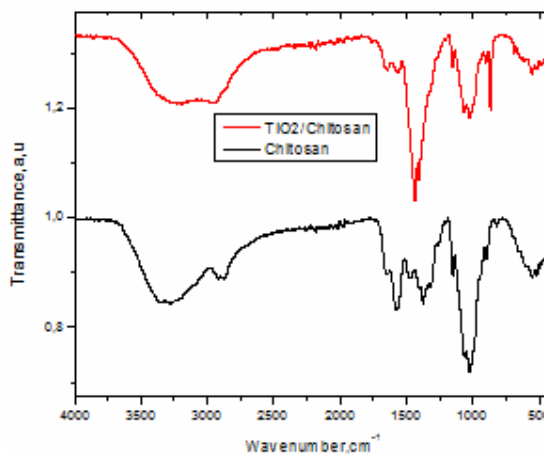


Figure 3: FTIR spectra of pure CS and TiO_2 -chitosan membrane

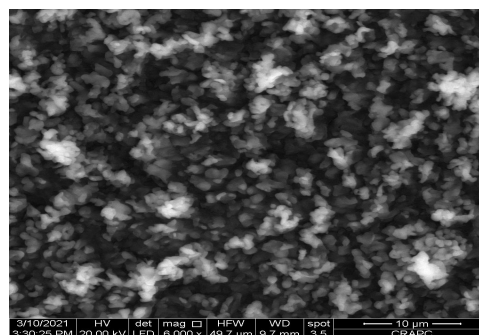
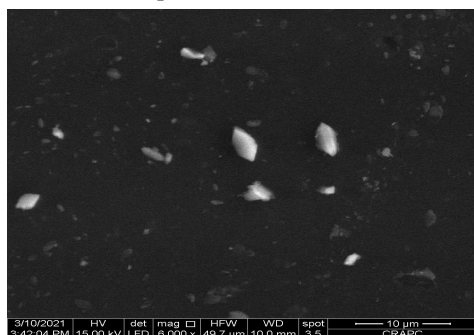


Figure 4: SEM images of pure CS and TiO_2 -Chitosan membrane

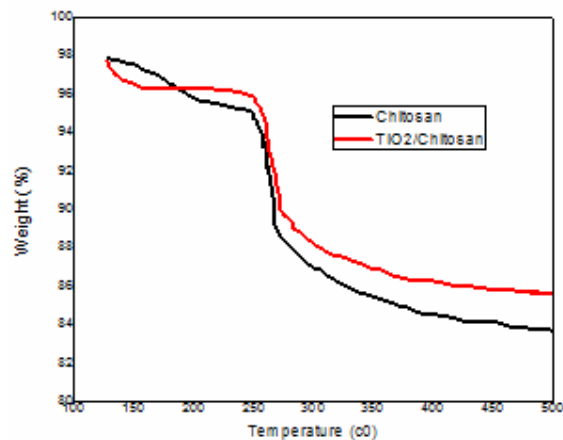


Figure 5: Thermogravimetric analysis (TGA) of pure CS and TiO_2 -Chitosan membranes

Table 2
Chemical and physical characteristics of the synthesized membranes

Membranes	Thickness, μm	Density, mg/cm^2	Water content, %	Contact angle, degrees
Chitosan	130	10.5	35.09	71
TiO ₂ -Chitosan	140	16.2	40.77	46

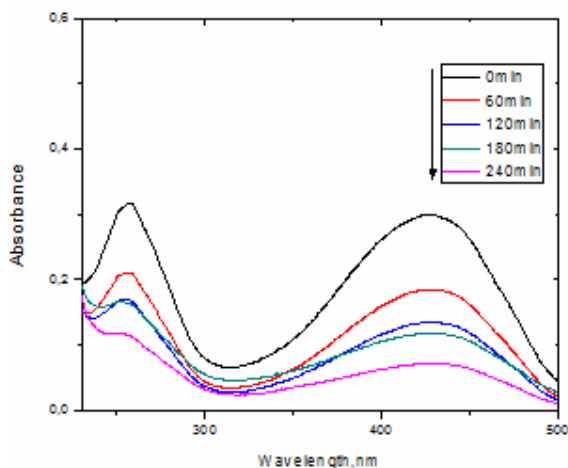


Figure 6: UV-Vis spectra of tartrazine degradation at different irradiation times under sun irradiation (10 mg/L, free pH (6), with TiO₂-chitosan membrane)

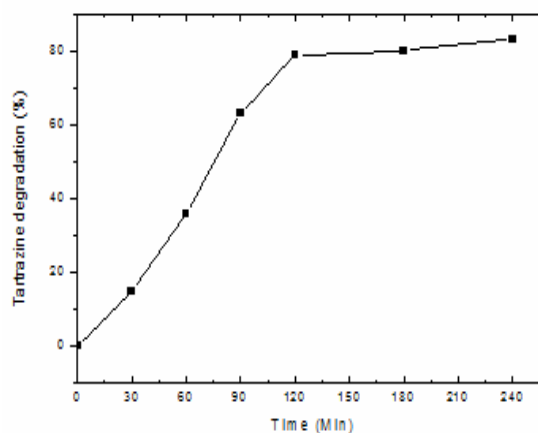


Figure 7: Effect of sunlight illumination time on photocatalytic degradation of tartrazine dye ($C_{\text{TAR}} = 10$ mg/L, and free pH = 6)

Photocatalytic activity experimental results

The photocatalytic treatment of simulated wastewater containing an azo dye was carried out using a TiO₂-CS membrane. Tartrazine dye was selected as a pollutant model.

The experiments were carried out using an open reactor of 250 mL directly exposed to solar light on a clear day. Aliquots of 3 mL, withdrawn at regular time intervals, were centrifuged to separate the solid particles from the aqueous solution. To determine the residual tartrazine dye concentration, a double-beam spectrophotometer (Shimadzu UV1800) was used at $\lambda_{\text{max}} = 427$ nm.

The photodegradation yield (R , %) is calculated as in the following equation (Eq. 1):^{3,7,21}

$$\text{Degradation (\%)} = \frac{C_0 - C_t}{C_0} \times 100 \quad (1)$$

where C_0 and C_t are the initial concentration of tartrazine and its concentration at time t , respectively.

The (UV-Vis) absorption spectrum of tartrazine (Fig. 6) presents two main bands: one in the near UV ($\lambda_{\text{max}} = 254$ nm) and another one in the visible range ($\lambda_{\text{max}} = 427$ nm) responsible for the yellow color. The band at 427 nm can be assigned to chromophore groups, and the 254 nm

band is characteristic of the individual aromatic rings. The decrease in the intensity of both peaks (254 and 427 nm) has been observed with time and with the changes in color of the tartrazine dye in the inset of Figure 6. The decrease is also meaningful with respect to the nitrogen to nitrogen double bond ($-\text{N}=\text{N}-$) of the azo dye, as the most active site for oxidative attack. These results are in harmony with similar work reported by Aoudjit *et al.*³

After 240 minutes, the bands (254 nm and 427 nm) disappeared. This disappearance of the bands indicates that the chromophore groups of tartrazine dye are broken down and opened by the attack of OH radicals. Thus, the tartrazine dye and aromatic intermediates were degraded into H₂O, CO₂ and mineral acids. The degradation of tartrazine under UV sun irradiation (intensity = 830 W/m²) was increased with increasing illumination time, as shown in Figure 7 (83% at the end of the reaction).

Stability and reusability of the TiO₂-Chitosan membrane

The stability of the TiO₂-Chitosan membrane was evaluated by XRD, FTIR and cycling

experiments. As can be seen from Figure 8, no difference was observed between the two XRD and FTIR spectra before and after recycling. This result indicates that the membrane exhibits constant properties before and after the degradation of tartrazine dye. As shown in Figure 9, although TiO₂-Chitosan still exhibited excellent photocatalytic activity for tartrazine degradation after 4 cycles, the efficiency decreased slightly

from 83 to 78%. This loss of photocatalytic efficiency (5% loss) is explained by the washing out of TiO₂ from the surface of the chitosan biopolymer during the first use and cleaning step, and these findings are consistent with previous research.^{2,3,7} It can be concluded that the TiO₂-Chitosan film has good chemical stability and potential for environmental remediation and industrial application.

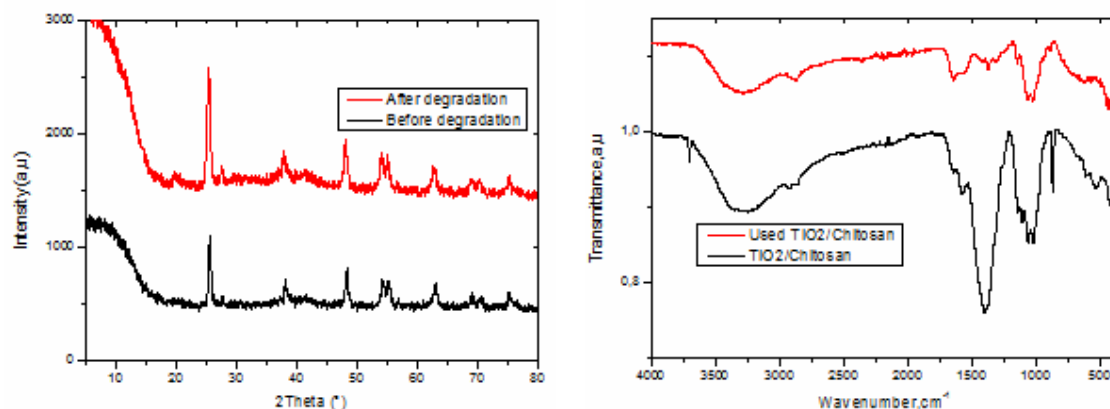


Figure 8: XRD patterns and FTIR spectra of TiO₂-Chitosan film before and after recycling

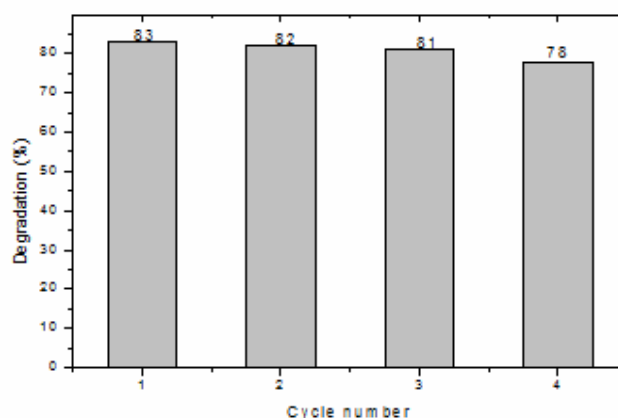


Figure 9: Photodegradation of tartrazine over four catalytic cycles in sunlight ($C_{\text{TAR}} = 10$ mg/L, and free pH = 6)

CONCLUSION

Developing highly efficient photocatalysts for water and wastewater treatment under sunlight irradiation is a promising approach to address the urgent demand for water remediation, particularly for the remediation of emerging pollutants, such as tartrazine dye. Thus, composite membranes based on TiO₂ and chitosan have been prepared and characterized, and their photocatalytic activity has been evaluated for the degradation of tartrazine under sunlight radiation. The maximum degradation efficiency of 83% was achieved with

an initial tartrazine concentration of 10 mg/L, at a free pH, and after 4 h of solar irradiation. After four consecutive uses, the degradation efficiency proved consistent, with an efficiency loss of 5%. The prepared TiO₂-Chitosan membranes are suitable for water remediation of tartrazine and related emerging pollutant contamination under solar irradiation.

ACKNOWLEDGEMENTS: This work was supported by the Solar Equipment Development Unit (UDES) Algeria.

REFERENCES

- ¹ T. Bouarroudj, L. Aoudjit, L. Djahida, B. Zaidi, M. Ouraghi *et al.*, *Water Sci. Technol.*, **83**, 2118 (2021), <https://doi.org/10.2166/wst.2021.106>
- ² L. Aoudjit, P. M. Martins, F. Madjene, D. Y. Petrovykh and S. Lanceros-Mendez, *J. Hazard. Mater.*, **344**, 408 (2018), <https://doi.org/10.1016/j.jhazmat.2017.10.053>
- ³ L. Aoudjit, D. Zioui, F. Touahra, S. Mahidine and K. Bachari, *Russ. J. Phys. Chem. A*, **95**, 1069 (2021), <https://doi.org/10.1134/S0036024421050034>
- ⁴ A. Sebti, F. Souahi, F. Mohellebi and S. Igoud, *Water Sci. Technol.*, **76**, 311 (2017), <https://doi.org/10.2166/wst.2017.201>
- ⁵ S. Igoud, D. Zeriri, L. Aoudjit, B. Boutra, A. Sebti *et al.*, *Irrig. Drain.*, **70**, 243 (2021), <https://doi.org/10.1002/ird.2540>
- ⁶ D. Zioui, H. Salazar, L. Aoudjit, P. M. Martins and S. Lanceros-Méndez, *Polymers*, **12**, 42 (2020), <https://doi.org/10.3390/polym12010042>
- ⁷ L. Aoudjit, H. Salazar, D. Zioui, A. Sebti, P. M. Martins *et al.*, *Polymers*, **13**, 3718 (2021), <https://doi.org/10.3390/polym13213718>
- ⁸ F. Ghribi, M. Sehalia, L. Aoudjit, F. Touahra, D. Zioui *et al.*, *J. Photochem. Photobiol. A*, **397**, 112510 (2020), <https://doi.org/10.1016/j.jphotochem.2020.112510>
- ⁹ S. Igoud, B. Boutra, L. Aoudjit, A. Sebti, F. Khene *et al.*, in *Procs. 7th International Renewable and Sustainable Energy Conference (IRSEC)*, 2019, p. 1, <https://doi.org/10.1109/IRSEC48032.2019.9078228>
- ¹⁰ F. Aoudjit, F. Touahra, L. Aoudjit, O. Cherifi and D. Halliche, *Water Sci. Technol.*, **82**, 2837 (2020), <https://doi.org/10.2166/wst.2020.519>
- ¹¹ A. Sebti, B. Boutra, M. Trari, L. Aoudjit and S. Igoud, in *Procs. International Conference in Artificial Intelligence in Renewable Energetic*, vol. 102, 2020, p. 143, <https://doi.org/10.1007/978-3-030-37207-1>
- ¹² D. Zioui, L. Aoudjit, Z. Tigrine, H. Aburideh and O. Arous, *Russ. J. Phys. Chem. A*, **96**, 1334 (2022), <https://doi.org/10.1134/S0036024422060334>
- ¹³ D. Zioui, L. Aoudjit, Z. Tigrine and H. Aburideh, *Cellulose Chem. Technol.*, **56**, 353 (2022), <https://doi.org/10.35812/CelluloseChemTechnol.2022.56.31>
- ¹⁴ H. Aburideh, Z. Tigrine, L. Aoudjit, Z. Belgroun, K. Redjimi *et al.*, *Cellulose Chem. Technol.*, **55**, 1153 (2021), <https://doi.org/10.35812/CelluloseChemTechnol.2021.55.99>
- ¹⁵ D. Zioui, O. Arous, N. Mameri, H. Kerdjoudj, M. San Sebastian *et al.*, *J. Hazard. Mater.*, **336**, 188 (2017), <https://doi.org/10.1016/j.jhazmat.2017.04.035>
- ¹⁶ W. Zhang, J. Chen, Y. Chen, W. Xia, Y. L. Xiong and H. Wang, *Carbohydr. Polym.*, **138**, 59 (2015), <https://doi.org/10.1016/j.carbpol.2015.11.031>
- ¹⁷ P. Kaewklin, U. Siripatrawan, A. Suwanagul and Y. S. Lee, *Biol. Macromol.*, **112**, 523 (2018), <https://doi.org/10.1016/j.ijbiomac.2018.01.124>
- ¹⁸ C. E. Zubieta, P. V. Messina, C. Luengo, M. Dennehy, O. Pieroni *et al.*, *J. Hazard. Mater.*, **152**, 765 (2008), <https://doi.org/10.1016/j.jhazmat.2007.07.043>
- ¹⁹ U. Habiba, T. A. Siddique, S. Talebian, J. L. Lee, A. Salleh *et al.*, *Int. J. Biol. Macromol.*, **177**, 32 (2017), <https://doi.org/10.1016/j.carbpol.2017.08.115>
- ²⁰ X. Zhang, G. Xiao, Y. Wang, Y. Zhao, H. Su *et al.*, *Carbohydr. Polym.*, **169**, 101 (2017), <https://doi.org/10.1016/j.carbpol.2017.03.073>
- ²¹ P. M. Martins, H. Salazar, L. Aoudjit, R. Gonçalves, D. Zioui *et al.*, *Chemosphere*, **262**, 128300 (2021), <https://doi.org/10.1016/j.chemosphere.2020.128300>